EUROPEAN ORGANIZATION FOR NUCLEAR RESEARCH

L3 Note 2734
March 20, 2002

Preliminary Results on the Measurement of Triple-Gauge-Boson Couplings of the W Boson at LEP

The L3 Collaboration

Abstract

We report on preliminary results on the measurement of triple-gauge-boson couplings of the W boson in e^+e^-collisions at LEP. Using semi-leptonic W-pair events measured in the L3 detector, we determine the couplings g_1^Z, κ_γ, λ_γ, g_5^Z, λ_Z and κ_Z. The measurements are combined with results obtained from the study of single-W production.

Imposing the constraints $\Delta\kappa_Z = \Delta g_1^Z - \Delta\kappa_\gamma \tan^2\theta_w$ and $\lambda_Z = \lambda_\gamma$, we obtain for the C and P conserving couplings the results: $\kappa_\gamma = 0.902 \pm 0.077(\text{stat.}) \pm 0.068(\text{syst.})$, $\lambda_\gamma = -0.030 \pm 0.047(\text{stat.}) \pm 0.029(\text{syst.})$ and $g_1^Z = 0.952 \pm 0.044(\text{stat.}) \pm 0.025(\text{syst.})$. All results are in agreement with the Standard-Model expectations.

Submitted to the *XXXVIIth Rencontres de Moriond*
ELECTROWEAK INTERACTIONS AND UNIFIED THEORIES
March 9-16, 2002, Les Arcs, France

1 Introduction

W-pair production and single-W production ($e^+e^- \rightarrow \mathrm{We}\nu$) all depend on the trilinear self couplings among the electroweak gauge bosons [1]. The existence of triple-gauge-boson vertices γWW and ZWW is predicted in the Standard Model as a consequence of the non-Abelian gauge structure of the electroweak theory [2].

To lowest order within the Standard Model [2] (SM), three Feynman diagrams contribute to W-pair production: the s-channel γ and Z-boson exchange and the t-channel ν_e exchange. The s-channel diagrams contain the γWW and ZWW vertices. The γWW vertex appears in one of the t-channel Feynman diagrams contributing to Weν production; at LEP2 centre-of-mass energies it dominates the corresponding diagram containing the ZWW vertex.

In general the vertices γWW and ZWW are parametrised in terms of seven triple-gauge-boson couplings (TGCs) each [3], too many to be measured simultaneously. Retaining only CP-conserving couplings and assuming electromagnetic gauge invariance, six TGCs remain, namely κ_γ, λ_γ, g_1^Z, g_5^Z, κ_Z and λ_Z. Within the SM, $g_1^\mathrm{Z} = \kappa_\gamma = \kappa_\mathrm{Z} = 1$ and $g_5^\mathrm{Z} = \lambda_\gamma = \lambda_\mathrm{Z} = 0$ at tree level. Except g_5^Z, these TGCs also conserve C and P separately.

The requirement of custodial SU(2) symmetry leads to the relations $\Delta\kappa_\mathrm{Z} = \Delta g_1^\mathrm{Z} - \Delta\kappa_\gamma \tan^2\theta_w$ and $\lambda_\mathrm{Z} = \lambda_\gamma$ [4–7], where Δ denotes the deviation of the TGC from its SM value and θ_w is the weak mixing angle.

When these constraints are applied, g_1^Z, κ_γ and λ_γ correspond to the operators in a linear realization of a gauge-invariant effective Lagrangian that do not affect the gauge-boson propagators at tree level [7]. The results shown below for g_1^Z, κ_γ and λ_γ are obtained assuming these constraints, whereas the results for g_5^Z, κ_Z and λ_Z are obtained without this assumption.

In this note we report on the measurement of these TGCs in the large data sample collected by the L3 detector in the years 1996-2000. They correspond to an integrated luminosity of 706 pb^{-1} at centre-of-mass energies in the range $\sqrt{s} = 161 - 208$ GeV.

The results are based on the analysis of multi-differential cross sections measured in semi-leptonic W-pair and single-W events. The single-W analysis is described elsewhere [8, 9], in this note we will only describe the combination procedure.

These preliminary results supersede our previous preliminary results [10] based on 1998 data collected at a centre-of-mass energy of 188.7 (189) GeV.

2 Analysis

The L3 detector is described in detail in Reference 11. The event selections used in this analysis are identical to those described in Reference 12.

Selection efficiencies and background contaminations of all processes are determined by Monte Carlo simulations. The following Monte Carlo event generators are used to simulate the signal and background reactions: YFSWW3 [13] and HERWIG [14] ($e^+e^- \rightarrow \mathrm{WW} \rightarrow ffff(\gamma)$); EXCALIBUR [15] ($e^+e^- \rightarrow ffff(\gamma)$); PYTHIA [16] ($e^+e^- \rightarrow q\bar{q}(\gamma), \mathrm{ZZ}(\gamma)$); KK2F [17] ($e^+e^- \rightarrow q\bar{q}(\gamma), \mu^+\mu^-(\gamma), \tau^+\tau^-(\gamma)$); KORALZ [18] ($e^+e^- \rightarrow \mu^+\mu^-(\gamma),\ \tau^+\tau^-(\gamma)$); BHAGENE3 [19], BHWIDE [20] and TEEGG [21] ($e^+e^- \rightarrow e^+e^-(\gamma)$), DIAG36 [22] and LEP4F [23] (leptonic two-photon collisions); PHOJET [24] (hadronic two-photon collisions). The response of the L3 detector is modeled with the GEANT [25] detector simulation program which includes the effects of energy loss, multiple scattering and showering in the detector materials and in the beam pipe.

The YFSWW3 program has been adopted as baseline Monte Carlo for signal processes. It includes $\mathcal{O}(\alpha)$ radiative corrections in the Leading Pole Approximation [26] which is believed to give a more accurate description of both the differential and total W-pair cross sections with respect to the KORALW [27] program used for our previous results (see Reference 28 for details and comparisons).

The selections reconstruct the visible fermions in the final state, *i.e.*, electrons, muons, τ jets corresponding to the visible τ decay products, and hadronic jets corresponding to quarks [29,30]. A kinematic fit is then performed to improve the resolution in the measured fermion energies and angles and to determine those not measured [31]. Four-momentum conservation and equal mass of the two W bosons are imposed as constraints. In $qq\tau\nu$ events, the energies of the two hadronic jets are rescaled by a common factor so that their sum equals half the centre-of-mass energy.

Summing over final-state fermion helicities, fixing the mass of the W boson and neglecting photon radiation, five phase-space angles completely describe the four-fermion final state from W-pair decay, for unpolarised initial states. These angles are the production angle of the W^- boson, Θ_{W^-}, and the polar and azimuthal decay angles in the rest systems of the two decaying W bosons, $\theta_\pm$ and $\phi_\pm$, for the fermion in W^- and the antifermion in W^+ decay. TGCs affect the total production cross section, the distribution of the W-boson production angle, and the polarisations of the two W bosons, which in turn determine the distributions of the W decay angles.

For charged leptons, the sign of their electric charge determines whether they are fermions or antifermions and the charge of the W boson. In $qq\ell\nu$ events the five-fold differential distribution in the W^- production angle, Θ_{W}, the two decay angles of the leptonically decaying W boson, θ_ℓ and ϕ_ℓ, and the two decay angles of the hadronically decaying W boson, θ_q and ϕ_q, are used for the determination of TGCs. To combine the distributions of ϕ_ℓ for leptons and antileptons, a shift of π is applied to ϕ_{ℓ^+}, since for CP conserving couplings differential cross sections are symmetric under the exchange $(\cos\theta_{\ell^-}, \phi_{\ell^-}) \leftrightarrow (\cos\theta_{\ell^+}, \phi_{\ell^+} + \pi)$.

For hadronic jets, the flavour of the original quarks are not measured. Thus, a two-fold ambiguity arises in the decay angles of hadronically decaying W bosons, namely $(\theta_q, \phi_q) \leftrightarrow (\pi - \theta_q, \pi + \phi_q)$. The ϕ_q distribution is therefore restricted to the interval $(0, \pi)$: the jet with $0 < \phi_q \leq \pi$ is assigned to the quark or the antiquark originated from the decay of W^- or W^+ respectively.

The distributions of the W^- production angle, Θ_{W}, and of $\cos\theta_\ell$, ϕ_ℓ, $\cos\theta_q$ and ϕ_q (W^+ and W^- combined) are shown in Figure 1 and Figure 2, respectively.

From the single-W analysis, the total cross sections, the lepton energy spectrum for the leptonic channel and the distribution of the neural-network output variable for the hadronic channel are used in the determination of TGCs. In order to avoid double counting, events selected by both the single-W and the W-pair selections, are only accounted for in the W-pair sample.

3 Fitting Procedure

For the data sample described above, Binned Maximum Likelihood (BML) fits are used to perform the TGC measurement. Likelihood functions are constructed based on the variables which have been introduced in Section 2. The phase-space spanned by these variables has dimension one for single-W events and dimension five in the case of semi-leptonic W-pairs.

The phase space is divided in bins and the likelihood is defined as the product of the Poisson probabilities of occupation of each bin. The likelihood for the k-th channel, as a function of a given set of couplings Ψ is given by:

$$L_k(\Psi) \quad = \quad \prod_{i}^{bins} \frac{e^{-\mu_i^k(\Psi)} \mu_i^k(\Psi)^{N_i^k}}{N_i^k!} \,, \tag{1}$$

where μ_i^k is the expected number of events in the i-th bin from the k-th channel and N_i^k is the corresponding observed number of events. The expected number of signal and background events per bin depend on the value of the couplings Ψ which are being fitted. This dependence is determined by a generator level reweighting procedure applied to fully simulated Monte Carlo events. For a value Ψ_{fit} varied during the fit, the weight R of the n-th event originally generated with TGC value Ψ_{gen} is calculated as the ratio:

$$R(p_n, \Psi_{\text{fit}}, \Psi_{\text{gen}}) \quad = \quad \frac{|\mathcal{M}(p_n, \Psi_{\text{fit}})|^2}{|\mathcal{M}(p_n, \Psi_{\text{gen}})|^2} \,, \tag{2}$$

where $\mathcal{M}$ is the matrix element of the final state considered, evaluated for the generated four-momenta p_n including radiated photons.

For single-W and WW events, matrix elements as implemented in the EXCALIBUR [15] event generator are used. In the case of W-pairs, the signal Monte Carlo is generated using YFSWW3, where only the CC03 set of diagrams is implemented. To correct for the missing diagrams, the matrix element in the numerator of Equation 2 is computed using the complete set of diagrams contributing to the four-fermion final state, while the one in the denominator contains only the CC03 diagrams.

The expected number of events in the i-th bin is written as the sum of signal and background contributions:

$$\mu_i(\Psi_{\text{fit}}) \quad = \quad \sum_{\text{sources}} \left(\frac{\sigma^{\text{gen}} \, \mathcal{L}}{N^{\text{gen}}} \cdot \sum_{j \in i-\text{th bin}} R(p_j, \Psi_{\text{fit}}, \Psi_{\text{gen}}) \right) \,, \tag{3}$$

where σ^{gen} denotes the cross section corresponding to the total Monte Carlo sample containing N^{gen} events for the sources considered (signal and background); $\mathcal{L}$ is the integrated luminosity. The sum extends over all accepted Monte Carlo events j which fall in the i-th bin. This takes detector effects and Ψ-dependent efficiencies and purities properly into account. For background sources which are independent of TGCs, each background event has a weight R equal to 1. Maximisation of the total likelihood function obtained by multiplying the likelihoods of all channels yields the result on the TGCs.

The fitting method described above determines the TGCs without any bias as long as the Monte Carlo describes photon radiation and detector effects such as resolution and acceptance functions correctly. The binning of the phase-space is chosen in such a way as to optimise the sensitivity within the limits set by the finite Monte Carlo statistics. The results of the fit are stable under variation of the binning used. The binnings used for the results presented are the following: for single-W, 40 bins between 0 and 200 GeV for the energy of the lepton and 50 bins for the neural network output between 0 and 1. For WW $\rightarrow q q \ell \nu$ we used 10 bins on $\cos \Theta_{\text{W}}$, 4 bins on $\cos \theta_l$ and ϕ_l and 3 bins on $\cos \theta_q$ and ϕ_q.

By fitting large Monte Carlo samples, typically a hundred times the size of the data, the fitting procedure is tested to high accuracy. The fits reproduce well the values of the TGCs of the large Monte Carlo samples being fitted, varied in a range corresponding to three times the error expected for the size of the data samples analysed. Also, the fit results do not depend on the values of the TGCs Ψ_{gen} of the Monte Carlo sample subjected to the reweighting procedure.

The reliability of the statistical errors as given by the fit is tested by fitting for each final state several hundreds of small Monte Carlo samples, each the size of the data samples. The width of the distribution of the fitted central values agrees well with the mean of the distribution of the fitted errors.

4 Systematic Uncertainties and Cross Checks

4.1 Systematic Error Studies

Systematic errors for the single-W results are dominated by the error on the background cross sections and the theoretical error on the signal cross section; they are evaluated as described in Reference 8 and amount to 0.08 for κ_γ and 0.11 for λ_γ.

The systematic uncertainties on the TGC measurement based on the W-pairs cross section analysis are summarised in Table 3. The largest contributions are due to the uncertainty in the modelling of charge reconstruction for leptons and jets and to the limited Monte Carlo statistics, with a relative importance which varies between the different couplings.

Possible systematic effects typically induce a shift in the maximum of the likelihood as well as a change of sensitivity. If the increase of fit error due to a variation of one of the systematic error sources is not balanced by a decrease of error for an opposite variation of that source, the difference of loss and gain of sensitivity is summed in quadrature to the shift to get the total systematic error. Sensitivity loss arises mainly due to uncertainties on the selection efficiencies and to the theoretical uncertainties on the $\mathrm{e^+e^-} \rightarrow \mathrm{WW}$ cross section.

An uncertainty of 0.5% on the theoretical $\mathrm{e^+e^-} \rightarrow \mathrm{WW}$ total cross section is assumed [28], based on the predictions of RacoonWW [32] and YFSWW3 [13]. Both programs implement improved $\mathcal{O}(\alpha)$ calculations using either LPA or Double Pole Approximation techniques. These improved calculations predict also a change in the slope of the $\cos\theta_{\mathrm{W}}$ distribution, one of the variables most sensitive to TGC's. The full effect of the change in slope is conservatively regarded as systematic uncertainty on the determination of TGC's.

The selection efficiencies of the separate WW subchannels have uncertainties which vary between 1.5% and 2.9% [33]. The influence of these uncertainties on the TGC measurement is evaluated by varying the expected cross section and the selection efficiencies in the specified range; uncertainties due to selection efficiencies of different final states are dominated by the selection procedure and are therefore treated as uncorrelated.

Lepton and jet charge assignment is needed for the correct reconstruction of the phase space angles. The agreement of data and Monte Carlo has been checked using Z peak calibration data with a statistical accuracy on the charge confusion probability varying between 0.6% and 1.2% depending on particle type and polar angle. Monte Carlo simulations are corrected for the residual difference with respect to data and the statistical uncertainty on this correction has been propagated in the fit in order to assign the corresponding systematic error.

Background cross sections and shapes have also been considered as possible sources of systematic effects. The cross sections of $\mathrm{q\bar{q}}(\gamma)$ and of ZZ backgrounds have been varied within the theoretical error of $\pm 5\%$ [28]. The slope of the two background sources have also been varied by 5% in the most sensitive variable, the cosine of the production angle of the W candidate. This was done to account for possible inaccuracies of the Monte Carlo prediction in the very restricted regions of phase space where the background processes are selected by the WW analysis.

A good description of Final State Radiation (FSR) is important to properly reconstruct the phase space variables used in the TGC fit. This effect was studied by repeating the TGC fit with Monte Carlo samples from which the events with FS photon of energy above a cutoff, varied between 100 MeV and 1 GeV, were removed.

Systematic effects due to the uncertainty on the measurement of W mass and width have been evaluated by generating a few high statistics Monte Carlo samples in which these parameters had been assigned different values. The resulting variation in the TGC measurement is rescaled to the one corresponding to the uncertainties on mass and width of the world average [34]. In a similar fashion the error due to the uncertainty on the LEP beam energy has been estimated to be negligible.

We test the agreement of data and Monte Carlo in the reconstruction of jet and lepton angles and energies by the use of di-jet and di-lepton events collected during Z peak calibration runs. The uncertainties on the calibrations of scales and resolutions of energy and angle measurements are propagated in the Monte Carlo and their effect on the TGC results is assigned as a systematic error.

High statistics Monte Carlo samples generated with different hadronisation schemes (JETSET [16], HERWIG [14] and ARIADNE [35]) are used to evaluate the effect of inaccurate modelling of hadronisation.

The uncertainty caused by limited Monte Carlo statistics was evaluated by repeating the TGC fit with subsets of the total reference sample, analysing the spread of the fit results as a function of the sample size and extrapolating this spread to the full sample size.

4.2 Optimal Observables Analysis of W-pair Events

For the W-pair data, an independent TGC analysis based on Optimal Observables (OO) was performed and used as a cross check of the binned maximum likelihood method. The WW differential cross section is a quadratic function of the anomalous couplings assumed to be real:

$$\frac{d\sigma}{d\vec{\Omega}} = c_0(\vec{\Omega}) + \sum_i c_{1,i}(\vec{\Omega})\,\psi_i + \sum_i \sum_j c_{2,ij}(\vec{\Omega})\,\psi_i \psi_j \tag{4}$$

where $\vec{\Omega} = (\Theta_W, \theta_+, \phi_+, \theta_-, \phi_-)$ are the phase-space angles introduced in Section 2 and ψ_i are the anomalous couplings considered. Optimal observables are defined as:

$$\mathcal{O}_{1,i} \equiv \frac{c_{1,i}(\vec{\Omega})}{c_0(\vec{\Omega})}\ ; \quad \mathcal{O}_{2,ij} \equiv \frac{c_{2,ij}(\vec{\Omega})}{c_0(\vec{\Omega})}\ . \tag{5}$$

These quantities contain the complete information about TGCs carried by $d\sigma/d\vec{\Omega}$, and therefore a fit to their distributions allows the determination of ψ_i with maximum precision [36].

When the deviations of anomalous couplings from zero are small, $\psi_i \sim 0$, quadratic terms in Equation 4 can be neglected. Therefore, only the variable $c_{1,i}(\vec{\Omega})/c_0(\vec{\Omega})$ is considered. The optimal observables are evaluated using the reconstructed four-momenta of the final state particles for both data and fully simulated Monte Carlo events; this new variable is close to the optimal one including detector effects. For hadronically decaying W bosons the two possible quark charge assignments are both taken into account with a weight 1/2. The dependence on the TGCs is evaluated using a generator level reweighting of Monte Carlo events similar to the one described in Section 3. Distributions of the first order optimal observables $\mathcal{O}_{1,i}$ for the couplings $\Delta\kappa_\gamma$, λ_γ and $\Delta g_1^{\rm Z}$, based on semi-leptonic WW data, are shown in Figure 3.

An extended unbinned maximum likelihood fit is used to extract the values of the couplings from the optimal observable distributions. The likelihood is multiplied by the Poissonian probability to obtain the number of events observed in the data given the accepted signal and background cross section and the integrated luminosity. The results of one-parameter fits to the couplings κ_γ, λ_γ and $g_1^{\rm Z}$, obtained imposing the constraints $\Delta\kappa_{\rm Z} = \Delta g_1^{\rm Z} - \Delta\kappa_\gamma \tan^2\theta_w$ and $\lambda_{\rm Z} = \lambda_\gamma$, and using semi-leptonic W-pair data for $\sqrt{s} \geq 189$ GeV are:

$$\kappa_\gamma = \quad 0.856^{+0.078}_{-0.086}\ \text{(OO)} \qquad \kappa_\gamma = \quad 0.780^{+0.074}_{-0.079}\ \text{(BML)} \tag{6}$$
$$\lambda_\gamma = -0.062^{+0.040}_{-0.036}\ \text{(OO)} \qquad \lambda_\gamma = -0.053^{+0.046}_{-0.043}\ \text{(BML)} \tag{7}$$
$$g_1^{\rm Z} = \quad 0.952^{+0.040}_{-0.034}\ \text{(OO)} \qquad g_1^{\rm Z} = \quad 0.934^{+0.043}_{-0.046}\ \text{(BML)} \tag{8}$$

where fit results and statistical errors are shown, for both optimal observables (OO) and binned maximum likelihood (BML) method. The comparison of the two methods shows good agreement of both central values and errors.

5 Results and Discussion

The results obtained from the study of W-pairs events collected at centre-of-mass energies from 161 GeV to 208 GeV have been combined, all data being reanalysed using the fit procedure discussed in Section 3.

The combination is done by taking into account correlations of systematic errors between data sets collected at different centre-of-mass energies. In Table 3 the estimated effect of different error sources on the determination of TGC's is shown.

To include the effect of systematic uncertainties in the log-likelihood curves, the curves are multiplied by scale factors of the form $\sigma^2/(\sigma^2+\delta^2)$, where σ is the statistical error and δ is the systematic error. This procedure is equivalent, in the Gaussian case, to the sum in quadrature of statistical and systematic errors.

The results of one-parameter fits, in which only one coupling is allowed to vary while the others are set to their Standard Model value, are shown in Table 1. Negative log-likelihood curves for the couplings $g_1^{\rm Z}$, κ_γ and λ_γ are shown in Figure 4.

In W-pair and single-W production, the triple-gauge-boson vertices are tested at different momentum-transfer scales Q^2: $Q^2 = s$ for W-pair production and $Q^2 = M_{\rm W}^2$ for single-W production.

No Q^2 dependence is observed. Compared to the current level of statistical accuracy, the Q^2 dependence of the TGCs expected in the SM is negligible [3] and is thus ignored in the combination.

The combination of semi-leptonic W-pairs data for the whole set of centre-of-mass energies and single-W data for $\sqrt{s} \leq 202$ GeV yields the following results for one-parameter fits:

$$\kappa_\gamma = \quad 0.902 \pm 0.077 \pm 0.068 \tag{9}$$
$$\lambda_\gamma = -0.030 \pm 0.047 \pm 0.030 \tag{10}$$
$$g_1^{\rm Z} = \quad 0.952 \pm 0.044 \pm 0.025\,. \tag{11}$$

The first error is statistical and the second systematic. The above results were obtained imposing the constraints $\Delta\kappa_{\rm Z} = \Delta g_1^{\rm Z} - \Delta\kappa_\gamma \tan^2\theta_w$ and $\lambda_{\rm Z} = \lambda_\gamma$ and fixing all other TGCs to their SM values. The contribution from W-pair production dominates in the case of λ_γ, while the single-W contribution is also important for the constraint on κ_γ. For the three remaining couplings, one-parameter fits to all semi-leptonic W-pair data result in:

$$g_5^{\mathrm{Z}} = 0.05 \pm 0.19 \pm 0.11 \tag{12}$$
$$\kappa_{\mathrm{Z}} = 0.84 \pm 0.07 \pm 0.05 \tag{13}$$
$$\lambda_{\mathrm{Z}} = 0.00 \pm 0.10 \pm 0.06\,. \tag{14}$$

Multi-parameter fits of TGCs are also performed, which allow for a more model-independent interpretation of the data. Fits to two of the couplings κ_γ, λ_γ and g_1^{Z}, keeping the third fixed at its SM value and a fit to all three of these TGCs are performed. In each case the constraints $\Delta\kappa_{\mathrm{Z}} = \Delta g_1^{\mathrm{Z}} - \Delta\kappa_\gamma \tan^2\theta_w$ and $\lambda_{\mathrm{Z}} = \lambda_\gamma$ are imposed. The numerical results of all multi-parameter fits to TGCs including the correlation coefficients are reported in Table 2.

The contour curves of 68% probability derived from fits to two of the three C- and P-conserving TGCs κ_γ, λ_γ and g_1^{Z}, keeping the third fixed at its SM value, are shown in Figure 5. The contour curves correspond to a change in log-likelihood of 1.15 with respect to its minimum. In the same plots contours derived from three-parameter fits are shown. They are obtained requiring the same log-likelihood change, but letting the third coupling free to vary in the fit. The comparison of contours derived from two- and three-parameter fits and the general agreement of the results of fits of different dimensionality show that there is no cancellation which would conceal the existence of anomalous couplings in low dimensional fits.

All single- and multi-parameter TGC results show good agreement with the SM expectation and confirm the existence of self-couplings among the electroweak gauge bosons.

6 Acknowledgements

We wish to congratulate the CERN accelerator divisions for the successful upgrade of the LEP machine and to express our gratitude for its good performance. We acknowledge with appreciation the effort of the engineers, technicians and support staff who have participated in the construction and maintenance of this experiment.

References

[1] F. Boudjema *et al.*, in *Physics at LEP 2*, Report CERN 96-01 (1996), eds G. Altarelli, T. Sjöstrand, F. Zwirner, Vol. 1, p. 207.

[2] S. L. Glashow, Nucl. Phys. **22** (1961) 579;
S. Weinberg, Phys. Rev. Lett. **19** (1967) 1264;
A. Salam, in *Elementary Particle Theory*, ed. N. Svartholm, Stockholm, Almquist and Wiksell (1968), 367.

[3] K. Hagiwara, R.D. Peccei, D. Zeppenfeld and K. Hikasa, Nucl. Phys. **B 282** (1987) 253.

[4] K. Gaemers and G. Gounaris, Z. Phys. **C 1** (1979) 259.

[5] M. Bilenky, J.L. Kneur, F.M. Renard and D. Schildknecht, Nucl. Phys. **B 409** (1993) 22; Nucl. Phys. **B 419** (1994) 240.

[6] I. Kuss and D. Schildknecht, Phys. Lett. **B 383** (1996) 470.

[7] G. Gounaris *et al.*, in *Physics at LEP 2*, Report CERN 96-01 (1996), eds G. Altarelli, T. Sjöstrand, F. Zwirner, Vol. 1, p. 525.

[8] The L3 Collaboration, M. Acciarri *et al.*, Phys. Lett. **B 487** (2000) 229.

[9] The L3 Collaboration, M. Acciarri *et al.*, *Preliminary Results on Single W Boson Production at 192 GeV* $\leq \sqrt{s} \leq$ *202 GeV*, L3 Note 2518 (2000).

[10] The L3 Collaboration, M. Acciarri *et al.*, *Preliminary Results on the Measurement of Triple-Gauge-Boson Couplings of the W Boson at LEP*, L3 Note 2378.

[11] The L3 Collaboration, B. Adeva *et al.*, Nucl. Instr. and Meth. **A 289** (1990) 35;
M. Chemarin *et al.*, Nucl. Instr. and Meth. **A 349** (1994) 345;
M. Acciarri *et al.*, Nucl. Instr. and Meth. **A 351** (1994) 300;
G. Basti *et al.*, Nucl. Instr. and Meth. **A 374** (1996) 293;
I.C. Brock *et al.*, Nucl. Instr. and Meth. **A 381** (1996) 236;
A. Adam *et al.*, Nucl. Instr. and Meth. **A 383** (1996) 342.

[12] The L3 Collaboration, M. Acciarri *et al.*, *Preliminary Results on the Measurements of W-Pair Cross Sections in* e^+e^- *Interactions at* $\sqrt{s} = 205 - 208$ *GeV and W-Decay Branching Fractions*, L3 Note 2638.

[13] YFSWW3 version 1.14 is used.
S. Jadach *et al.*, Phys. Rev. **D 54** (1996) 5434; Phys. Lett. **B 417** (1998) 326; Phys. Rev. **D 61** (2000) 113010; hep-ph/0007012.

[14] The HERWIG version 5.9 is used.
G. Marchesini and B. Webber, Nucl. Phys. **B 310** (1988) 461;
I.G. Knowles, Nucl. Phys. **B 310** (1988) 571;
G. Marchesini *et al.*, Comp. Phys. Comm. **67** (1992) 465.

[15] F.A. Berends, R. Kleiss and R. Pittau, Nucl. Phys. **B 424** (1994) 308; Nucl. Phys. **B 426** (1994) 344; Nucl. Phys. (Proc. Suppl.) **B 37** (1994) 163;
R. Kleiss and R. Pittau, Comp. Phys. Comm. **83** (1994) 141;
R. Pittau, Phys. Lett. **B 335** (1994) 490.

[16] PYTHIA versions 5.722 and 6.1 are used.
T. Sjöstrand, *PYTHIA 5.7 and JETSET 7.4 Physics and Manual*,
CERN-TH/7112/93 (1993), revised August 1995; Comp. Phys. Comm. **82** (1994) 74; hep-ph/0001032.

[17] S. Jadach, B.F.L. Ward and Z. Wąs, Phys. Lett. **B 449** (1999) 97.

[18] The KORALZ version 4.03 is used.
S. Jadach, B. F. L. Ward and Z. Wąs, Comp. Phys. Comm. **79** (1994) 503.

[19] J.H. Field, Phys. Lett. **B 323** (1994) 432;
J.H. Field and T. Riemann, Comp. Phys. Comm. **94** (1996) 53.

[20] BHWIDE version 1.01 is used.
S. Jadach, W. Placzek, B.F.L. Ward, Phys. Rev. **D 40** (1989) 3582, Comp. Phys. Comm. **70** (1992) 305, Phys. Lett. **B 390** (1997) 298.

[21] D. Karlen, Nucl. Phys. **B 289** (1987) 23.

[22] F. A. Berends, P. H. Daverfeldt and R. Kleiss, Nucl. Phys. **B 253** (1985) 441.

[23] J.A.M. Vermaseren, J. Smith and G. Grammer Jr, Phys. Rev. **D 19** (1979) 137;
J.A.M. Vermaseren, Nucl. Phys. **B 229** (1983) 347.

[24] PHOJET version 1.05 is used.
R. Engel, Z. Phys. **C 66** (1995) 203; R. Engel and J. Ranft, Phys. Rev. **D 54** (1996) 4244.

[25] The L3 detector simulation is based on GEANT Version 3.15.
R. Brun *et al.*, *GEANT 3*, CERN-DD/EE/84-1 (Revised), 1987.
The GHEISHA program (H. Fesefeldt, RWTH Aachen Report PITHA 85/02 (1985)) is used to simulate hadronic interactions.

[26] W. Beenakker, F.A. Berends and A.P. Chapovsky, Nucl. Phys. **B 548** (1999) 3.

[27] The KORALW version 1.33 is used.
M. Skrzypek, S. Jadach, W. Placzek and Z. Wąs, Comp. Phys. Comm. **94** (1996) 216;
M. Skrzypek, S. Jadach, M. Martinez, W. Placzek and Z. Wąs, Phys. Lett. **B 372** (1996) 289.

[28] M. W. Grünewald *et al.*, in *Reports of the Working Groups on Precision Calculations for LEP2 Physics*, Report CERN 2000-009 (2000), eds S. Jadach, G. Passarino and R. Pittau, p. 1.

[29] The L3 Collaboration, M. Acciarri *et al.*, Phys. Lett. **B 398** (1997) 223.

[30] The L3 Collaboration, M. Acciarri *et al.*, Phys. Lett. **B 407** (1997) 419.

[31] The L3 Collaboration, M. Acciarri *et al.*, Phys. Lett. **B 413** (1997) 176.

[32] A. Denner *et al.*, Phys. Lett. **B 475** (2000) 127; Nucl. Phys. **B 587** (2000) 67.

[33] The L3 Collaboration, M. Acciarri *et al.*, Phys. Lett. **B 496** (2000) 19.

[34] D.E. Groom *et al.*, *The 2000 Review of Particle Physics*, Eur. Phys. J. **C 15** (2000) 1.

[35] L. Lönnblad, Comp. Phys. Comm. **71** (1992) 15.

[36] G.K. Fanourakis, D. Fassouliotis and S.E. Tzamarias, Nucl. Instr. and Meth. **A 414** (1998) 399.

Fit parameter	κ_γ	λ_γ	g_1^Z
Weν 130-202 GeV	$1.08^{+0.11}_{-0.11} \pm 0.08$	$0.12^{+0.25}_{-0.41} \pm 0.11$	-
WW 161-208 GeV	$0.780 \pm 0.075 \pm 0.072$	$-0.031 \pm 0.047 \pm 0.030$	$0.952 \pm 0.044 \pm 0.025$
All channels combined	$0.902 \pm 0.077 \pm 0.068$	$-0.030 \pm 0.047 \pm 0.030$	$0.952 \pm 0.044 \pm 0.025$
SM value	1.0	0.0	1.0

Fit parameter	g_5^Z	κ_Z	λ_Z
WW 161-208 GeV	$0.05 \pm 0.19 \pm 0.11$	$0.84 \pm 0.07 \pm 0.05$	$0.00 \pm 0.10 \pm 0.06$
SM value	0.0	1.0	0.0

Table 1: Results of one-parameter fits to the TGCs κ_γ, λ_γ, g_1^Z, g_5^Z, κ_Z and λ_Z based on single-W and semi-leptonic W-pair events, and their combination. The single-W results are obtained after removing the events which were already selected as W-pair. All results are at 68% C.L.. For each TGC fit, all other parameters are set to their SM values; for the set κ_γ, λ_γ and g_1^Z the constraints $\Delta\kappa_Z = \Delta g_1^Z - \Delta\kappa_\gamma \tan^2\theta_w$ and $\lambda_Z = \lambda_\gamma$ are imposed. The first error is statistical, the second systematic.

Fit parameter	SM value	Results (68% CL)	Results (95% CL)	correlation coeffs. κ_γ	λ_γ	g_1^Z
two-parameter fits						
κ_γ	1.0	$0.898^{+0.088}_{-0.105}$	(0.70; 1.24)	1.00	-	-0.29
g_1^Z	1.0	$0.970^{+0.060}_{-0.057}$	(0.83; 1.08)		-	1.00
λ_γ	0.0	$0.107^{+0.068}_{-0.097}$	(-0.12; 0.23)	-	1.00	-0.79
g_1^Z	1.0	$0.847^{+0.088}_{-0.061}$	(0.74; 1.07)	-		1.00
κ_γ	1.0	$0.899^{+0.090}_{-0.103}$	(0.70; 1.13)	1.00	-0.24	-
λ_γ	0.0	$-0.014^{+0.062}_{-0.056}$	(-0.12; 0.11)		1.00	-
three-parameter fit						
κ_γ	1.0	$0.90^{+0.26}_{-0.10}$	(0.71; 1.31)	1.00	-0.45	0.27
λ_γ	0.0	$0.02^{+0.17}_{-0.08}$	(-0.14; 0.26)		1.00	-0.88
g_1^Z	1.0	$0.96^{+0.08}_{-0.19}$	(0.71; 1.11)			1.00

Table 2: Results of two- and three-parameter fits of the couplings κ_γ, λ_γ and g_1^Z with the constraints $\Delta\kappa_Z = \Delta g_1^Z - \Delta\kappa_\gamma \tan^2\theta_w$ and $\lambda_Z = \lambda_\gamma$ imposed; all other couplings are set to their SM values. Correlation coefficients are also shown. These results are obtained from the combination of all the data analysed; systematic errors are included.

Error source	Systematic error on		
	g_1^{Z}	κ_γ	λ_γ
Error on Selection efficiencies	0.007	0.021	0.007
Charge confusion	0.010	0.031	0.015
Jet and lepton measurement	0.004	0.027	0.009
Monte Carlo statistics	0.013	0.021	0.014
Uncertainty on total σ	0.004	0.012	0.005
$\mathcal{O}(\alpha)$ correction	0.006	0.047	0.009
Background σ and shape	0.006	0.005	0.009
FSR	0.009	0.003	0.005
W mass and width	0.010	0.015	0.012
Fragmentation	0.004	0.003	0.002
Total systematic error	0.025	0.072	0.030

Table 3: Systematic errors for the fit of TGC based on semi-leptonic W-pairs. For each coupling the errors are obtained in one-parameter fits, by setting all other couplings to their SM value. The constraints $\Delta\kappa_{\mathrm{Z}} = \Delta g_1^{\mathrm{Z}} - \Delta\kappa_\gamma \tan^2\theta_w$ and $\lambda_{\mathrm{Z}} = \lambda_\gamma$ are imposed. All results are preliminary.

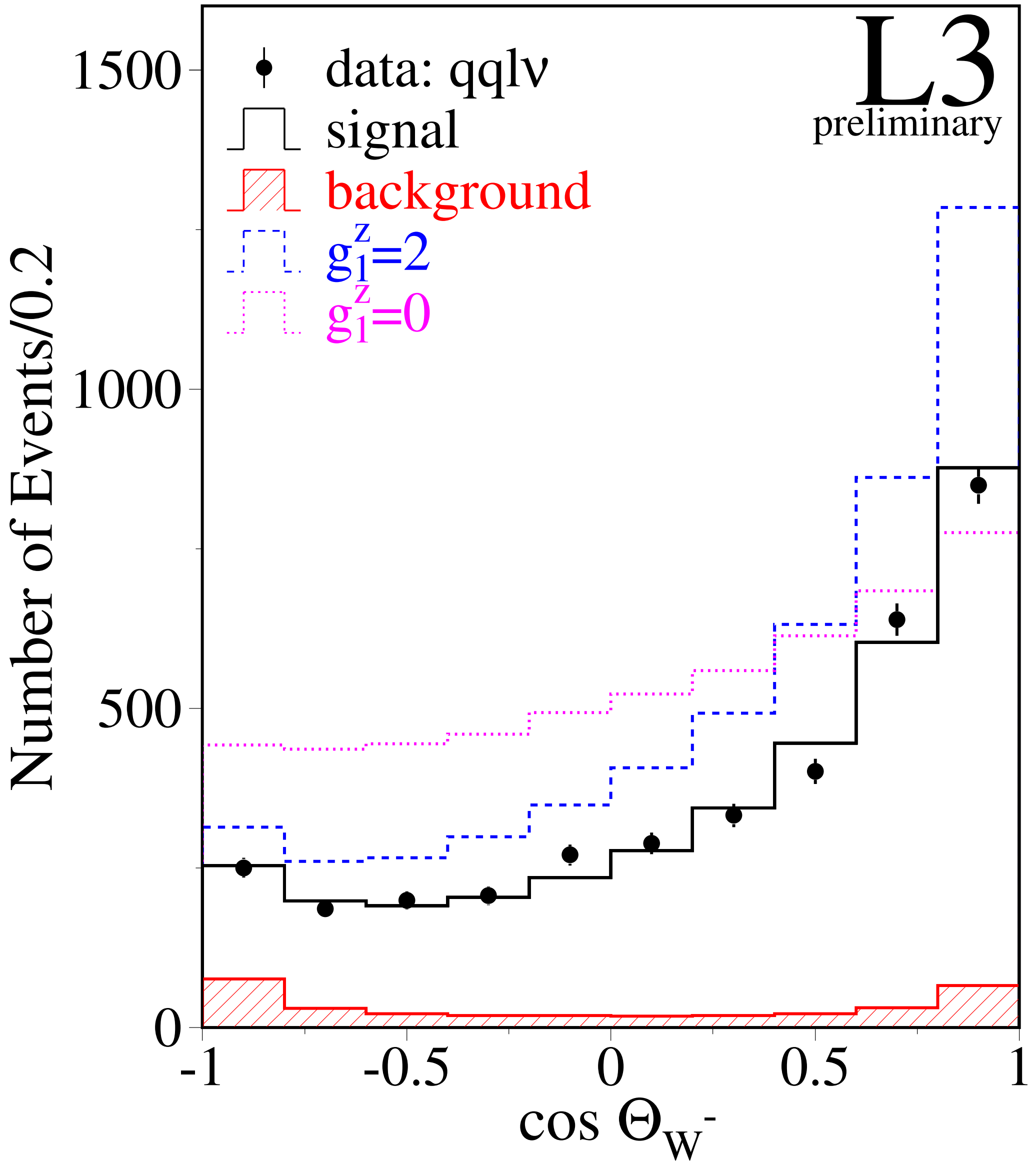

Figure 1: Distribution of the reconstructed production angle, $\cos\Theta_{\mathrm{W}^-}$, of the W^- boson in W-pair events for $qq\ell\nu$ events. The data collected at $\sqrt{s} = 189 - 208$ GeV are shown, together with the expectations for the SM ($g_1^{\mathrm{Z}} = 1$), and for anomalous TGCs ($g_1^{\mathrm{Z}} = 0$ or 2).

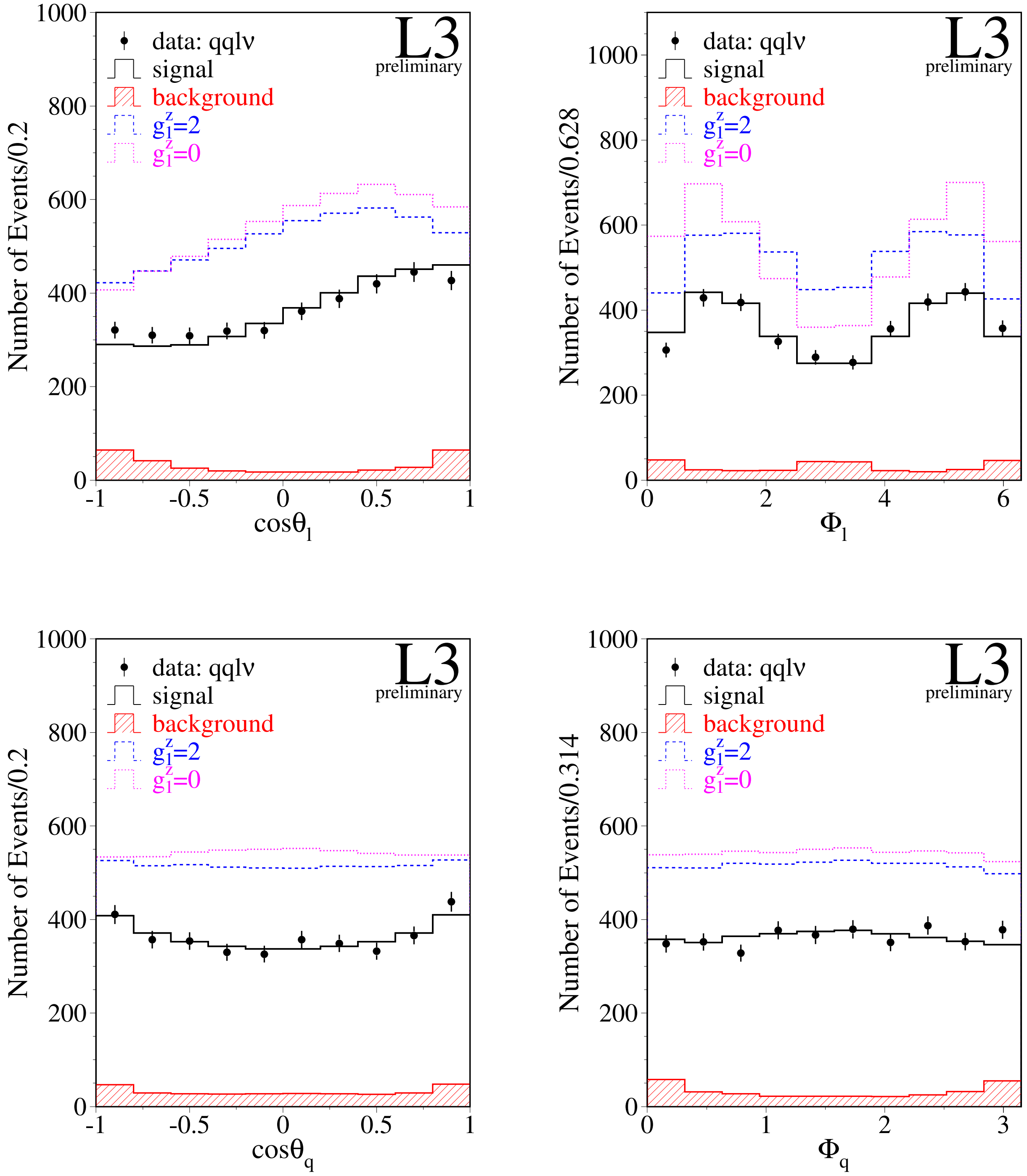

Figure 2: Distributions of the reconstructed W decay angles in $qq\ell\nu$ W-pair events. The phase space angles of the lepton (antilepton), $\cos\theta_\ell$ and ϕ_ℓ, are shown in the upper left and upper right plots, respectively. The decay angles of the hadronically decaying W, $\cos\theta_q$ and ϕ_q are shown in the lower left and lower right plots, respectively. The ϕ_q distributions is plotted in the interval $(0,\pi)$ due to the quark charge ambiguity. The data collected at $\sqrt{s} = 189 - 208$ GeV are shown, together with the expectations for the SM ($g_1^Z = 1$), and for anomalous TGCs, ($g_1^Z = 0$ or 2).

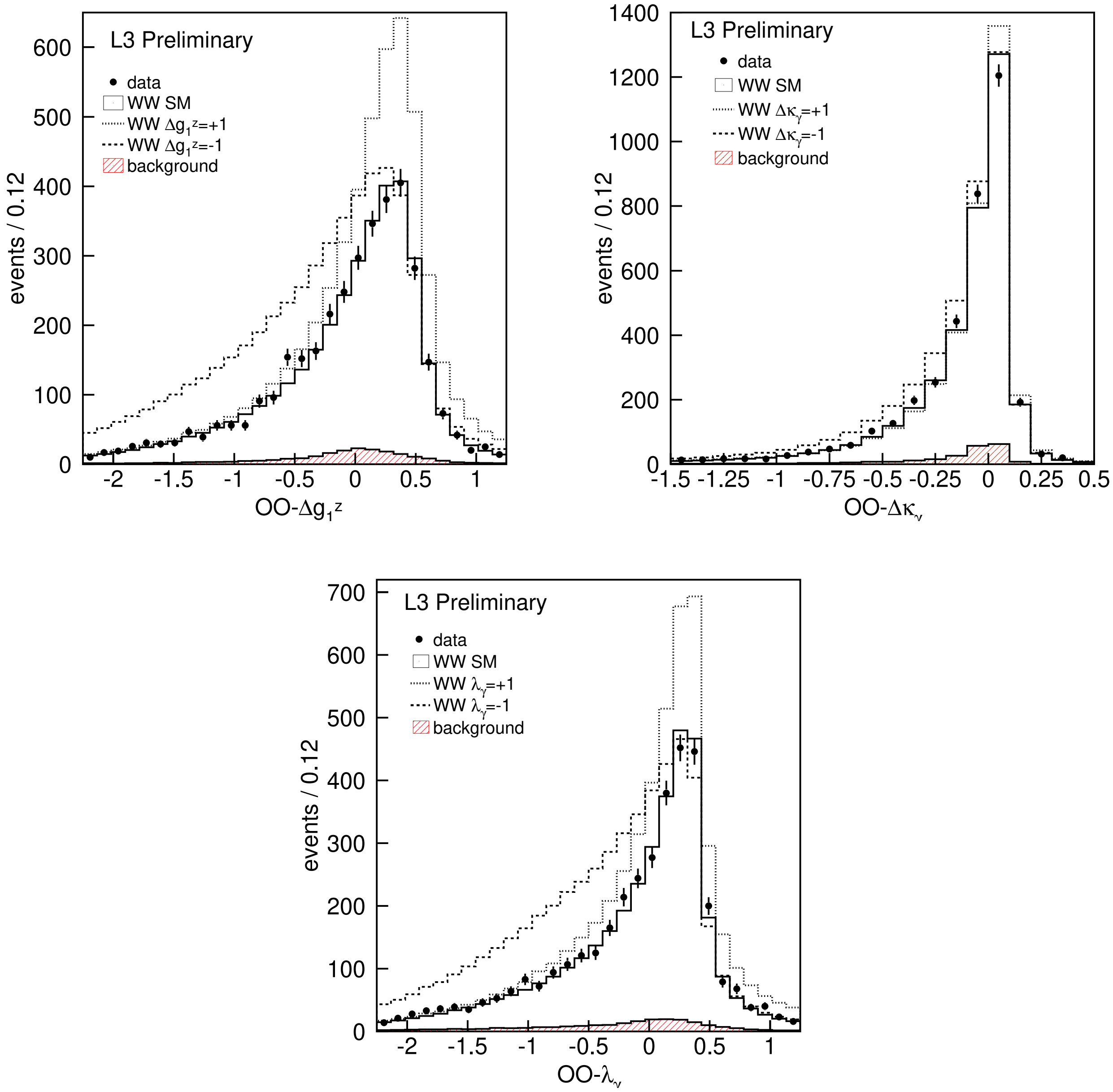

Figure 3: Distributions of the first order optimal observables for the anomalous couplings Δg_1^Z, $\Delta\kappa_\gamma$ and λ_γ. The semi-leptonic WW data collected at $\sqrt{s} = 189-208$ GeV are shown, together with the expectations for the SM, and for anomalous TGCs.

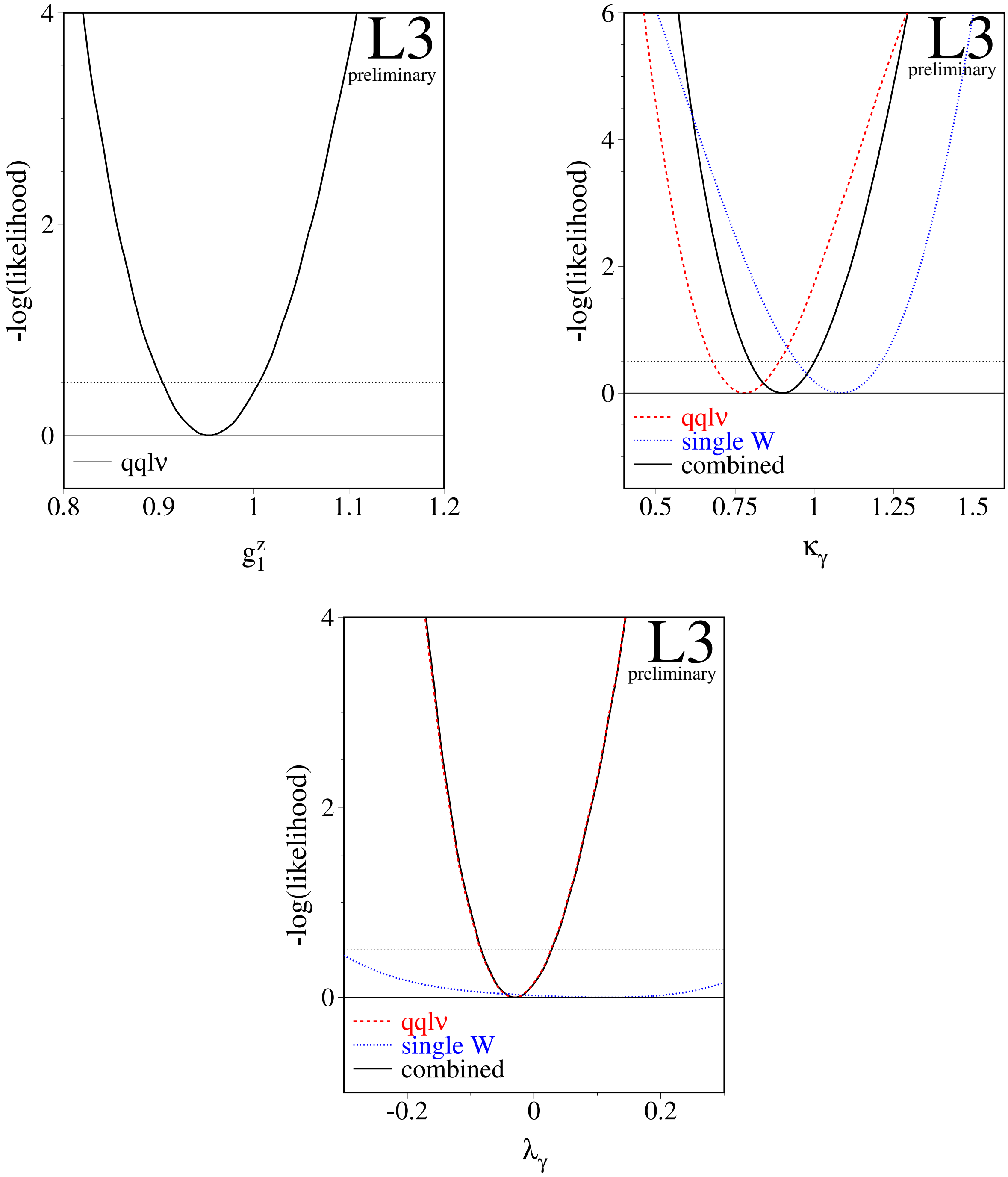

Figure 4: Negative log-likelihood functions (including statistical and systematic errors) for one-parameter fits to the TGCs: g_1^{Z}, κ_γ and λ_γ. The constraints $\Delta\kappa_{\mathrm{Z}} = \Delta g_1^{\mathrm{Z}} - \Delta\kappa_\gamma \tan^2\theta_w$ and $\lambda_{\mathrm{Z}} = \lambda_\gamma$ are imposed.

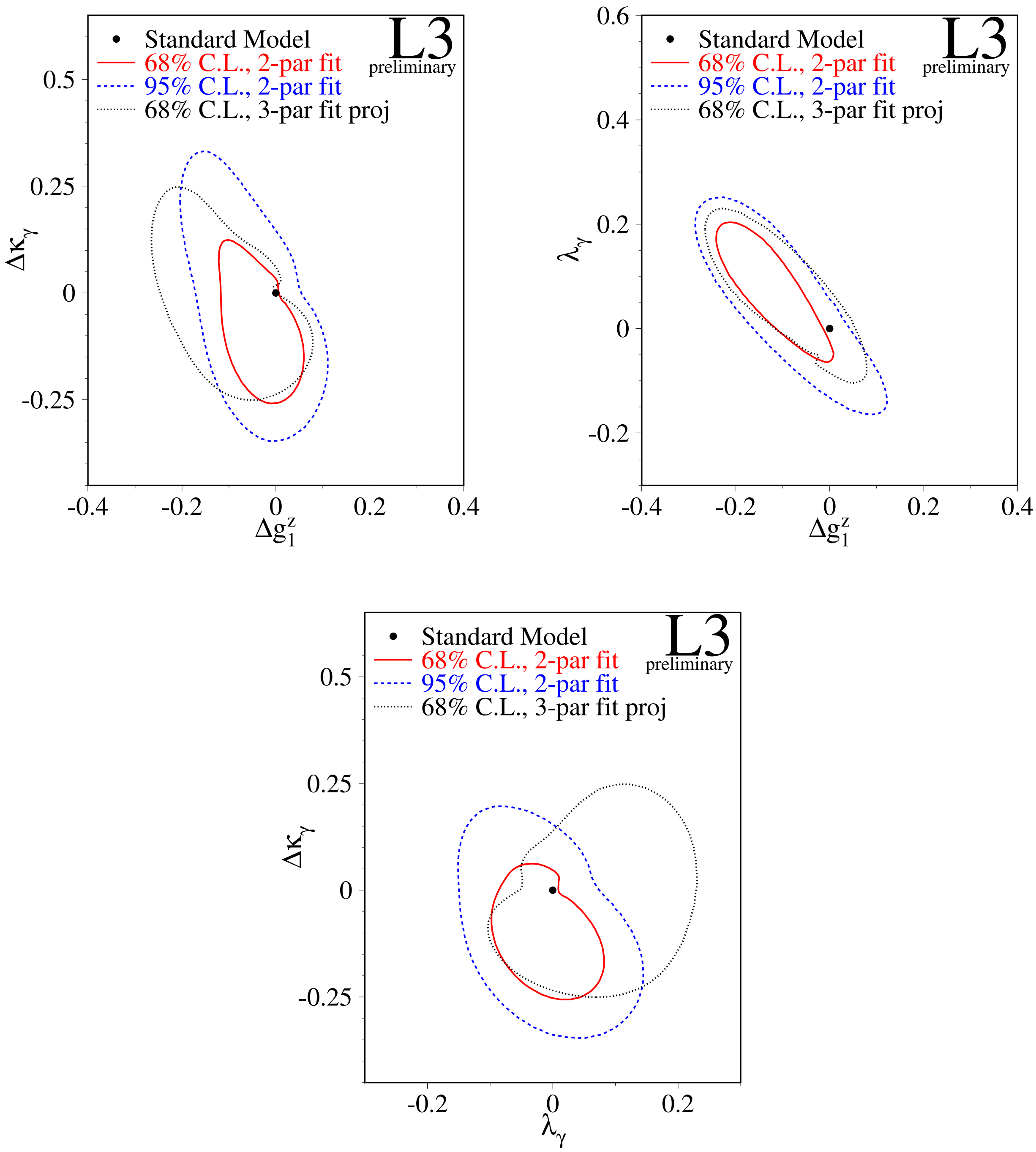

Figure 5: Contour curves of 68% probability for the two-parameter fits to the TGCs (full lines): g_1^Z and κ_γ with $\lambda_\gamma = 0$, g_1^Z and λ_γ with $\kappa_\gamma = 1$, and κ_γ and λ_γ with $g_1^Z = 1$. The contour curves at 95% (dashed lines) are also given. The dotted lines represent two-dimensional projections of the 3-parameter log-likelihood, obtained by requiring a variation of the log-likelihood of 1.15 from the minimum, letting the third coupling free in the fit. The constraints $\Delta\kappa_Z = \Delta g_1^Z - \Delta\kappa_\gamma \tan^2\theta_w$ and $\lambda_Z = \lambda_\gamma$ are imposed and all other couplings are set to their SM value. Systematic errors are included.